Design and Performance of a 46-m-High MSE wall

Article *in* Journal of Geotechnical and Geoenvironmental Engineering · June 2010

DOI: 10.1061/(ASCE)GT.1943-5606.0000294

6 authors, including:

Armin Stuedlein
Oregon State University

William J. Neely

Design and Performance of a 46-m-High MSE Wall

Armin W. Stuedlein, Ph.D., P.E., M.ASCE[1]; Michael Bailey, P.E., M.ASCE[2]; Doug Lindquist, P.E., M.ASCE[3]; John Sankey, P.E., M.ASCE[4]; and William J. Neely, Ph.D., P.E., M.ASCE[5]

Abstract: This paper focuses on the design and performance of a very tall mechanically stabilized earth (MSE) wall. Expansion of Seattle-Tacoma International Airport called for the construction of a third runway west of the two existing runways. A significant volume of compacted earth fill was required to raise the grade as much as 50 m to meet the level of the existing airfield. Nominal 2H:1V fill slopes were used where possible, but MSE retaining walls were used where fill slopes would have encroached into existing wetlands. Consequently a four-tier 46-m-tall MSE wall was constructed along a portion of the western edge of the embankment. Performance monitoring included strain gauge-instrumented reinforcing strips, inclinometer installations with sondex settlement rings, optical survey of the wall facing for vertical and lateral movements, and piezometers. This paper describes wall design issues, aspects associated with the instrumentation of the wall, and the observed performance. Monitoring indicates satisfactory performance of the MSE wall and compares reasonably well with predicted performance.

DOI: 10.1061/(ASCE)GT.1943-5606.0000294

CE Database subject headings: Soil stabilization; Retaining walls; Performance characteristics; Instrumentation; Design; Displacement; Washington; Airport and airfield runways.

Author keywords: Soil stabilization; Retaining walls; Performance; Instrumentation; Design; Displacement.

Introduction

The familiarity and acceptance of mechanically stabilized earth (MSE) systems with engineers continues to increase as performance data of constructed walls become available. Specifically, the design and construction of tall MSE walls (greater than 25 m) are proliferating worldwide due to increasing restrictions of right of way, wetlands, and other space-limiting conditions (Sankey and Soliman 2004). Expansion of the Seattle-Tacoma International Airport (STIA) included the construction of three MSE walls for the third runway embankment, including the single-tier 17.7-m (58-ft)-high south MSE wall, the near vertical two-tier 25.9-m (85-ft)-high north wall, and the near vertical four-tier 45.7-m (150-ft)-high west MSE wall. Another three MSE walls up to 16 m (53 ft) tall were constructed for other parts of the airport improvements (note that these heights refer to the total reinforced height including toe embedment and exposed face). The north and west MSE walls were instrumented for construction performance monitoring. The performance data provided additional insight into the behavior of the two tallest MSE walls during and immediately after construction. This paper focuses on the design, instrumentation, and performance of the tallest of the two walls monitored, that is, the 45.7-m west MSE wall.

Project Background

The Port of Seattle owns and operates STIA, located south of Seattle. Prior to construction of the third runway the Federal Aviation Administration limited operations to just one of the two existing runways for arrivals during inclement weather due to the limited distance between the existing runways.

The centerline of the new third runway is located approximately 760-m (2,500-ft) west of the existing second runway to allow greater flexibility to air traffic control operations. The length of the new runway is approximately 2.6 km (8,500 ft), which excludes the north and south safety areas. In order to raise the grade to match the elevation of the airfield, a 13×10^6 m^3 (17×10^6 yd^3) zoned embankment fill was constructed. Although embankment side slopes of 2H:1V were allowed for much of the filling, adjacent creeks and tributary wetlands limited the extent of the embankment in some locations. Prior to selecting tall MSE walls, the design team considered eight different types of retaining walls and more than 60 wall/slope geometric configurations to increase land use area while limiting encroachment into adjacent creeks and wetlands. This review led to the selection of MSE walls using galvanized high-adherence steel strip reinforcements, granular select backfill, and cruciform-shaped precast concrete facing panels.

The west MSE wall, which forms part of the western boundary of the third runway embankment, required the construction of an approximately 436-m (1,430-ft)-long, four-tier, MSE wall up to

[1]Assistant Professor, School of Civil and Construction Engineering, Oregon State Univ., 220 Owen Hall, Corvallis, OR 97331 (corresponding author). E-mail: armin.stuedlein@oregonstate.edu

[2]CEO, Hart Crowser, 1700 Westlake Ave. North, Ste. 200, Seattle, WA 98109. E-mail: mike.bailey@hartcrowser.com

[3]Senior Associate, Hart Crowser, 1700 Westlake Ave. North, Ste. 200, Seattle, WA 98109. E-mail: doug.lindquist@hartcrowser.com

[4]Vice President of Engineering, The Reinforced Earth Company, 8614 Westwood Center Dr., Vienna, VA 22182. E-mail: jsankey@reinforcedearth.com

[5]Senior Vice President and Chief Engineer, Retaining Wall Services, Inc., 1660 Hotel Circle North, Suite 304, San Diego, CA 92108. E-mail: wneely@retainingwallservices.com

Note. This manuscript was submitted on April 10, 2009; approved on November 21, 2009; published online on May 14, 2010. Discussion period open until November 1, 2010; separate discussions must be submitted for individual papers. This paper is part of the ***Journal of Geotechnical and Geoenvironmental Engineering***, Vol. 136, No. 6, June 1, 2010. ©ASCE, ISSN 1090-0241/2010/6-786–796/$25.00.

Fig. 1. Perspective aerial photo of the new third runway at STIA viewed from the northwest and showing the north and west MSE walls

45.7 m (150 ft) tall (Fig. 1). The total area of wall face was approximately 12,100 m^2 (130,200 ft^2). The exposed height of the MSE wall is 41.9 m (137.5 ft) at this section. Based on an extensive literature review, this wall is believed to be the tallest MSE wall in the western hemisphere.

Site and Subsurface Conditions

The preconstruction topography of the project site is generally characterized by gentle rolling drumlins and recessional outwash, the product of extensive glaciation of the Puget Sound Lowland. The last glaciation, termed the Vashon Stade of the Frasier Glaciation, occurred approximately 10,000–20,000 years ago with ice thicknesses reaching 1,000 m (3,000 ft) in the vicinity of Seattle (Galster and LaPrade 1991). Glacially overridden material, in the form of advance outwash and glacial till, is typically found at depths of less than 10 m in the vicinity of STIA. Surficial soils include Pleistocene recessional outwash and Holocene alluvium and lacustrine deposits.

The tallest portion of the west MSE wall occupies an area previously serving as a seasonal drainage tributary to Miller Creek. The wall was constructed to avoid having to relocate the creek; wetland enhancements were required elsewhere to compensate for the impacted wetland areas. In general, the subsurface conditions below the footprint of the west MSE wall prior to construction comprised 3–4 m (10–12 ft) of soft peat, interlayered with loose to medium dense silty sand and sandy peat, over glacially overridden dense to very dense, slightly gravelly, silty to very silty sand. Shallow perched groundwater followed the surface of the glacially overridden soils.

Selected Aspects of MSE Wall Design

The west MSE wall, like other MSE walls at STIA, required that special attention be given to certain design aspects (Stuedlein et al. 2007; Sankey et al. 2007). Challenges in designing and constructing such a tall MSE wall for a 100-year design life included the following: (1) structural MSE considerations associated with soil reinforcing strips and facing elements, (2) geotechnical considerations such as weak, compressible, and potentially liquefiable foundation soils in an active regional seismic setting, and (3) the overall wall performance objectives. Local community groups opposed to airport expansion claimed that no MSE wall had been built to such heights and that the seismic risk made the project infeasible; geotechnical issues were raised in an attempt to intervene in the construction permit process. The Port of Seattle and the design team established a technical review board of internationally recognized geotechnical experts to provide an independent technical appraisal of all aspects of embankment and wall design. Selected aspects of the wall design are presented here.

Ground Improvement

Shallow subsurface soil and groundwater conditions indicated the potential for lateral instability and excess differential settlements below the MSE fill. A significant ground improvement test program was undertaken to determine if subgrade reinforcement and in situ densification would provide acceptable support and avoid the need for overexcavation and replacement. The ground improvement test program consisted of installation of bottom feed stone columns or aggregate piers of varying diameters and spacing followed by testing the matrix soil for increases in penetration resistance using both standard penetration test and cone penetration test. The test program demonstrated that insufficient improvement was realized and that excavation and replacement of the unsuitable soils would be required (Chen and Bailey 2004). The unsuitable subgrade (relatively compressible, low shear strength, and potentially liquefiable surficial soils) was excavated to a depth of up to 4 m to the top of the dense to very dense glacially overridden soils and replaced with densely compacted granular backfill to provide a high strength foundation for the MSE wall. Backfill in the subgrade improvement zone consisted of clean sandy gravel and gravelly sand with less than 3% fines (material passing the U.S. No. 200 sieve) based on the fraction passing the 19-mm (3/4-in.) sieve. The field acceptance criterion for the backfill was a minimum compaction of 95% of maximum modified Proctor dry density per ASTM D 1557.

Above the subgrade improvement zone, a drainage blanket of 0.6 m (2 ft) minimum thickness was placed and compacted below the MSE wall footprint and adjacent embankment fill. The drainage layer provides hydraulic relief for existing seeps covered by the embankment, preventing infiltration into the embankment. Specifications for the drainage material were the same as the subgrade replacement fill.

Overall MSE Wall Design

After reviewing the current standards of practice, the design team selected the AASHTO Standard Specifications for Highway Bridges (AASHTO 1996 and Interim Updates) as the basis for design. Given the proposed height of the MSE walls, the design team incorporated additional design measures based on the experience of the selected wall designer, as well as deformation modeling and compound stability analyses of the reinforced soil structures by Port's geotechnical consultant.

Geotechnical site exploration and design were accomplished by Crowser. The MSE soil reinforcement and concrete panel design were completed by The Reinforced Earth Company (RECo), with global and compound stability independently evaluated by Crowser using limit equilibrium and deformation analyses of the MSE walls and embankment for static and seismic conditions. The use of limit equilibrium and deformation analyses is briefly described, followed by a comparison of measured and predicted performance.

Reinforced Fill

Reinforced fill specifications called for well graded granular fill material within the gradation range shown in Table 1, with no

Table 1. Gradation Requirements for Reinforced Fill

Sieve size (mm)	Minimum percent passing	Maximum percent passing
100 (4 in.)	100	—
19 (3/4 in.)	70	100
4.76 (U.S. number 4)	40	80
0.297 (U.S. number 50)	0	40
0.074 (U.S. number 200)	0	5[a]

[a]Based on material passing 19 mm (3/4-in.) sieve.

plastic fines. The gradation and plastic limits are more restrictive than the AASHTO design criteria for MSE walls [i.e., percent fines < 15 and plastic index (PI) < 6]. The fill was required to meet these stricter criteria to minimize potential metal loss of the reinforcing strips and exceed minimum shear strength requirements. The fill came from sources meeting stringent environmental criteria intended to avoid potential water quality impacts in the adjacent wetlands. Prospective bidders were required to identify proposed fill material sources and provide supporting laboratory analyses as part of their bid. In addition to meeting gradation and electrochemical requirements, contractor-proposed material submittals required direct shear test (305-mm square box per ASTM D 3080) results to verify that fill in the reinforced zone would meet or exceed the minimum friction angle of 37°. The contractor was required by specification to shear soil used for the reinforced fill zone at normal stresses ranging from 175 to 550 kPa (from 25 to 80 psi) at a minimum of 92% maximum modified Proctor dry density. Direct shear tests performed under these conditions provided mean and standard deviation of peak friction angles of 41° and 2.4°, respectively, for soil used in the reinforced zone. The test specimens were characterized with mean and standard deviation of moist unit weights of 20.5 and 0.9 kN/m^3 (130.5 and 5.9 pcf), respectively, and mean and standard deviation of optimum moisture contents of 10.6 and 2.1%, respectively. Field compaction data indicated typical in-place unit weights of 22 kN/m^3 (140 pcf).

Except near the wall face, the specifications required reinforced fill to be compacted to a minimum of 92% of maximum modified Proctor dry density and within ±2% of optimum moisture content per ASTM D 1557 or to a higher density as needed to meet or exceed the density of the specimens used for the qualifying shear strength tests. The specifications also required the fill material in the reinforced zone to be compacted in 305-mm (12-in.)-thick lifts or less as needed to accommodate the vertical reinforcement spacing. Within 0.9–1.5 m (3–5 ft) of the precast concrete facing panels, compaction was restricted to prevent undue deflection of the wall face.

Reinforcement Design

The highest MSE walls incorporated several tiers mainly for aesthetic reasons. The west MSE wall is approximately 436 m (1,430 ft) long, consists of four tiers, and is 45.7 m (150 ft) high at the tallest section (Figs. 1 and 2). The maximum exposed height of the MSE wall is 41.9 m (137.5 ft), not including the unreinforced soil slope "surcharge" above the top of the wall. This 2H:1V soil slope reaches a crest height of 4.5 m (15 ft) above the top of the wall.

Design of the ribbed steel reinforcing strips was accomplished by RECo to satisfy the internal stability requirements for the reinforced soil mass. Strip lengths were evaluated on a tier-by-tier

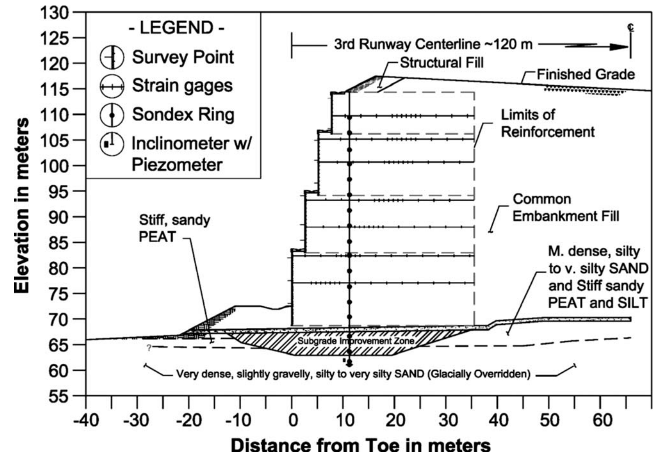

Fig. 2. West MSE wall cross section with typical instrumentation

basis for the west MSE wall and maintained at a minimum of 70% of the overlying wall height. Evaluations were made for strip pullout, resistance and tensile capacity, sliding, and overturning for both static and seismic conditions. The high-adherence reinforcing strip is an efficient soil load transfer device because granular soil particles are compacted between and against the faces of the ribs. Horizontal stresses are transferred to the steel by direct bearing of soil against the rib faces, and movement of the strips is resisted by soil-to-soil friction across the tops of the ribs rather than by soil-to-steel contact along the top and bottom surfaces of the strip. Additionally, because of restrained dilatancy near the strips there are localized increases in effective normal stress at the soil-to-strip interface and a corresponding increase in shearing resistance (Jewell et al. 1985). The soil-to-steel interaction creates a coherent but relatively flexible structure in which the reinforcing strip pullout resistance is of greater importance in the upper 6 m of the structure and tensile capacity of the strips is more important at greater depths. Though evaluations indicated shorter reinforcing strips length could be considered in many portions of the MSE wall; the AASHTO criterion for minimum length was followed because of the critical nature of the structure.

Design of the steel reinforcing strips included a metal loss allowance for the 100-year design life of the MSE wall. The ribbed steel strips were 50 mm (1.97 in.) wide by 6 mm (0.24 in.) thick, with a nominal yield stress of 448 MPa (65 ksi). RECo anticipated 1.01 mm (0.04 in.) of metal loss per side over the assumed 100-year design life. The reduced section (i.e., after section loss) was used in both internal stability analyses and compound stability analyses. Initial reinforcing design for portions of the wall included some strips 4 mm in thickness due to smaller loads near the top of the wall; this was subsequently modified to the use of 6-mm strips throughout based on the results of the compound stability analyses.

The maximum reinforcing strip lengths for the first, second, third, and fourth tiers of the west MSE wall are 35.4 (116), 32.9 (108), 30.5 (100), and 28 m (92 ft) long, respectively. The tiers were offset laterally 2.44 m (8 ft) from one another for aesthetic reasons; however, recent research indicates that offsetting tiers may reduce the reinforcement tensions (Leshchinsky and Han 2004). The vertical reinforcement strip spacing ranged from 0.24 to 0.78 m (from 0.79 to 2.56 ft)/row, with 34, 16, 16, and 11 rows for the first, second, third, and fourth tiers, respectively. Horizontal reinforcement strip spacing ranged from 0.14 to 0.74 m (from 0.46 to 2.43 ft). Internal stability analyses and numeric modeling were performed to check that static and dynamic tensile stresses in the reinforcement do not typically exceed 55% of the nominal yield stress throughout the 100-year design life.

Seismic Considerations

Ground Motions

The Port of Seattle and its design consultants selected the seismic design level as an event with a 10% probability of exceedance in 50 years. At the time of design, the hazard associated with this event was considered standard for highway bridges (AASHTO 1996) and for other structures not deemed to be lifeline structures. The performance criteria for the MSE wall during and subsequent to shaking were (1) to remain stable with reinforcement stresses typically less than 55% of yield stress and total displacement less than 1 m (3.3 ft), (2) to prevent impact to nearby creeks and wetlands due to shaking of the MSE walls, and (3) to prevent operational impacts to the new runway due to the design earthquake. A site-specific probabilistic seismic hazard analysis (PSHA) was performed to identify the nearby seismic sources and level of seismic hazard at the site and was supplemented by a deterministic seismic hazard analysis (DSHA) of rupture of the Seattle Fault, a large potential source located 11 km (7 miles) north of the airport. The results of the probabilistic and deterministic seismic analyses were used to obtain the peak ground acceleration (PGA) and design response spectrum. Four single component ground motions were selected to reflect the magnitude, duration, and frequency content consistent with the PSHA and one ground motion was selected to represent the DSHA. The selected ground motions were then scaled in the frequency domain to match their design response spectrum. Because of the larger hazard calculated in the DSHA, this motion was used in subsequent analyses.

Site Response Analyses

The critical (DSHA) ground motion was used as input for one-dimensional (1D) and two-dimensional (2D) site response analyses. The commercially available software Proshake (Proshake user manual 2000) was used in the initial stages of design; following the refinement of subsurface and embankment design parameters, 1D analyses were rerun and supplemented with 2D site response analyses performed using QUAD4M (Idriss et al. 1973; Hudson et al. 1994). Fourteen cross sections were evaluated for various sloped embankment and MSE wall cross sections; the three west MSE wall sections evaluated represented exposed wall heights of 12.2, 27.4, and 42.7 m and included the benched service road in front and sloped fill above the MSE wall. The QUAD4M analysis results were used as input to the limit equilibrium and deformation-based analyses. Time histories of equivalent horizontal acceleration were obtained by spatially integrating the inertial forces acting on potentially unstable "soil blocks" (Fig. 3) and dividing the total resultant force by the mass of the block (Seed and Martin 1966; Bray et al. 1995). The peak horizontal acceleration for each of the blocks analyzed was then used in critical slip-surface-specific pseudostatic limit equilibrium and sliding block analyses of Newmark (1965). In general, the results of the site response analyses indicated that (1) the 1D site response analyses produced cyclic shear stress time histories that were more conservative than the 2D site response analyses and (2) the accelerations were higher for shorter walls than for taller walls indicating deamplification of acceleration with increasing MSE wall height.

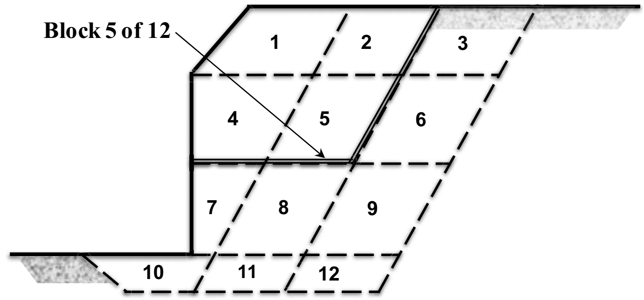

Fig. 3. Conceptual sketch of typical soil block model for the determination of yield acceleration and sliding block displacement analyses

Stability Analyses

Limit equilibrium pseudostatic internal and external stability analyses were performed by RECo. A PGA of 0.38 g was selected for the assessment of external overturning and sliding stability following AASHTO codes, with target factors of safety (FSs) of 1.5 and 1.1, respectively. The FSs calculated for the west MSE wall were 1.56 and 1.29 for overturning and sliding, respectively.

Compound and global stability of the MSE wall was performed by Crowser using limit equilibrium pseudostatic and postearthquake residual strength analyses. Methods of Spencer (1967) and Morgenstern and Price (1965) were used with both circular and block slip surfaces combined with a grid and radius search routine. The reinforcing strips were modeled as anchors (User's guide, slope/W for stability analysis, version 4 1998), with an allowable bond resistance calculated as a function of the pullout resistance factor, overburden stress, strip density per layer, and strip cross section. The seismic hazard selected for assessing compound and global stability corresponded to one-half of the peak equivalent horizontal acceleration developed using the 2D analyses as described above. This value typically ranged from 0.16 to 0.20 (i.e., PGA of 0.32–0.40 g) depending on the amplification or deamplification calculated in QUAD4 based on the location of the critical slip surface in relation to the corresponding soil block (Fig. 3). Where the target FS for global stability was not met subgrade improvement zones or reinforcement strip density was modified to achieve a satisfactory FS. The FS computed for critical compound and global slip surfaces corresponding to the final design geometry and subgrade improvements ranged from 1.12 to 1.44, exceeding the target FS of 1.1 recommended by Elias et al. (2001). The yield acceleration corresponding to the soil blocks exhibiting the largest displacement ranged from 0.36 to 0.46 g for the west MSE wall; this information was used in Newmark-based displacement analyses.

Sliding Block Displacement Analyses

Six wall sections, each with 10–18 blocks of soil (e.g., Fig. 3), were evaluated along the length of the west MSE wall. Following the calculation of a yield acceleration for each block of soil at a given wall section, displacements were evaluated using the sliding block double integration of Newmark (1965) and the procedures of Makdisi and Seed (1978). The maximum acceleration value used with the Makdisi-Seed method was determined from the equivalent horizontal acceleration time histories described previously. These procedures resulted in a number of seismic displacement estimates, the largest of which was approximately 10 mm for the west MSE wall. The displacement-based analyses were supplemented with numerical modeling.

Displacement-Based Numerical Modeling

Displacement-based modeling of the west wall was used to assess performance independent of the pseudostatic limit equilibrium analyses called for in AASHTO. The purpose of the modeling was to verify design based on the AASHTO code rather than to optimize the wall design. An additional benefit of the displacement-based numerical modeling was that it enabled checking the sensitivity of predicted displacements to the timing of liquefaction triggering relative to the start and end of shaking. A finite difference model, FLAC v4.0 [Fast LaGrangian Analysis of Continua (FLAC), version 4.0 2000] was selected for 2D modeling of the MSE wall.

The finite difference model had a height of 67 m (220 ft) and a width of 168 m (550 ft). Modeling the reinforced zone of soil required balancing the need for accurate modeling of problem geometry with the practical need for a reasonable dynamic solution time. Rather than model every layer of soil reinforcement, the design team decided to model the reinforcement strips with a single composite strip located at the center of each of the 31 face panels in the vertical section; each composite reinforcement strip was modeled with an area of steel equivalent to the 4–25 strips per panel. The steel reinforcements were individually scaled and distributed on a unit width basis. For the purpose of assessing reinforcement stresses during seismic simulation, the area of reinforcing strips was reduced by the maximum design metal loss (i.e., approximately a 33% reduction in steel). To reduce the number of simulations, the smaller area was also used for the end-of-construction modeling, the results of which are presented herein. The reinforcing strips were modeled using the 1D cable structural element in FLAC, which uses springs to represent axial stiffness and shear stiffness, and a slider for interface bond strength for each internodal segment. The bond strength of the cable element can be modeled with either adhesion, friction, or both; adhesion was neglected for this study.

Acceleration time histories were extracted from the QUAD4M models at an elevation corresponding to the base of the FLAC model and applied to the FLAC model as seismic input. Various seismic cases considering different times for liquefaction triggering were evaluated using the model. Based on these analyses, a maximum displacement of approximately 0.3 m was calculated, corresponding to the case where liquefaction was triggered at the beginning of shaking, outside the subgrade improvement zone, and in front of the MSE wall. This displacement exceeded the approximately 0.1-m displacement obtained when liquefaction was neglected and was slightly larger than the model with liquefaction occurring following ground shaking. The liquefaction effects were primarily caused by the liquefiable soils located below the embankment outside of the subgrade improvement zone. Because the subgrade improvement zone extended up to 15 m outside the footprint of the MSE wall, liquefaction triggering in front of the wall did not significantly affect the seismic response of the wall. Refer to Lindquist (2008) for a detailed discussion of the FLAC model, including the static and dynamic soil properties, soil constitutive models, steel and concrete material parameters used, and model results.

Instrumentation of the West MSE Wall

Geotechnical instrumentation and observational method (Peck 1969) are critical to extrapolate design of engineered facilities beyond the scale commonly constructed and to verify and support improvement of design methods and instrumentation techniques [e.g., Stuedlein et al. (2004, 2007) and Negussey and Stuedlein (2003)]. The objective of the monitoring program was to evaluate wall performance during and at the end of construction. Performance was observed by monitoring displacements of the wall face, foundation soils and retained soils, tensile strains and inferred stresses in the reinforcing strips, and piezometric levels. "Red flag" criteria for the performance data, presented by Stuedlein et al. (2007), were developed so that the design team could immediately address any performance problem or data that appeared suspect (e.g., unanticipated, omitted, or erroneous). An observation that was red-flagged triggered immediate action to determine the cause and assess the need for remedial action. Refer to Stuedlein et al. (2007) for a complete description of the types of instrumentation, the data acquisition system, and the criteria for flagging data employed on the project.

Displacement Monitoring Points

The west wall was fitted with 68 survey targets, termed displacement monitoring points (DMPs), which were grouped in varying numbers corresponding to the number of tiers at 10 separate wall stations. The monitoring stations were horizontally separated from one another by approximately 38 m (125 ft) on average, with a greater concentration of monitoring stations along the portion of the wall with the greatest height and where tier end points resulted in significant height changes. The DMPs were surveyed optically using a "total station" instrument, with observations specified to meet accuracy and resolution of 3 mm (0.01 ft) and 0.3 mm (0.001 ft), respectively.

Inclinometers

Seven inclinometer installations were established at three stations; two stations were instrumented with an array of three inclinometers and one station with one inclinometer. The single inclinometer casing was located near the maximum height of the wall, approximately 2 m behind the top tier face (see Fig. 2), with two arrays of three inclinometers located on either side of the single casing at a distance of about 95 m (310 ft). The first lengths of inclinometer casing were initially installed in boreholes prior to wall construction and were extended vertically as fill construction proceeded. Anticipating some compression of the casing due to filling, the instrumentation subcontractor installed 4-mm-wide stainless steel bands at 3-m (10-ft)-depth intervals for sondex measurements in addition to a telescoping section of inclinometer casing.

Piezometers

Seven vibrating wire piezometers were placed in fully grouted boreholes, each about 3 m (10 ft) away from a corresponding inclinometer installation. Changes in elevation of the shallow groundwater were not unexpected and occurred on a transitory basis due to typical Puget Sound rainfall. The need for any action due to groundwater changes was not anticipated, but the designers wanted real-time accurate groundwater elevation information available for any stability analysis that might become necessary based on other instrumentation data. The piezometers showed no significant response due to the placement of the embankment and wall; therefore, the data are not presented herein.

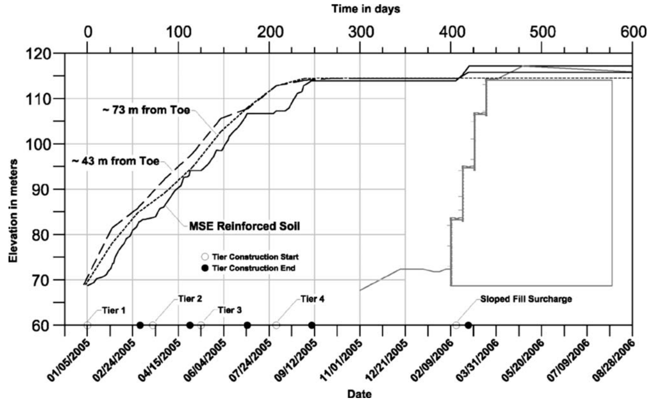

Fig. 4. West MSE wall fill placement time history

Instrumented Reinforcing Strips

Two sections of instrumented reinforcing strips, spaced approximately 4 m (13 ft) apart, were installed in the west MSE wall to provide redundancy and improve the reliability of the measurements. Instrumented reinforcing strips consisted of 13–16 strain gauge pairs (i.e., gages placed top and bottom of the reinforcement at each gauge location) along the strips. The gages were more closely spaced near the locations of anticipated peak strain for enhanced resolution. Fig. 2 shows the location of each instrumented reinforcing strip and strip-specific gauge pair distribution for a typical instrumented section. Refer to Stuedlein et al. (2007) for a discussion of the preparation and installation of gages on the reinforcing strips.

Construction of the West MSE Wall

Filling Time History

Construction of the third runway embankment occurred intermittently in phases over an 8-year time period ending in November 2006. Prior to constructing the west MSE wall, the main embankment fill directly east of the wall had been in place for about 1 year. The excavation of unsuitable subgrade material and its replacement with compacted structural fill below the west MSE wall occurred during the Summer and Fall of 2004. Fig. 4 shows the filling time history for the west MSE wall and at two locations approximately 43 and 73 m behind the wall. Construction of the west MSE wall began January 5, 2005, with the first, 14.6-m (48-ft)-tall, tier completed 58 days later. Construction of the second, 11.7-m (38.4-ft)-high, tier of the MSE wall began on day 72 and took 41 days to complete. Tiers 3 and 4 began on days 132 and 205 and required 44 and 42 days to complete to heights of 11.5 and 7.9 m (37.7 and 26 ft), respectively. Final grading operations brought the overall third runway embankment in the area of the west MSE wall to design elevation at the beginning of 2006. This activity included the placement of the sloped fill above the west MSE wall, which occurred between days 406–420.

Construction Crews, Methods, and Equipment

Construction of the west MSE wall was accomplished using three separate crews: a facing panel crew, a reinforcing strip crew, and a backfilling crew. A lead foreman painted the proper reinforcing strip lengths on the back of the panels, checked panel installations from the front and back at the end of the shift to ensure they were installed in the proper location, and performed quality control checks on vertical and horizontal alignments.

A typical panel crew included an equipment operator who managed the lay-down yard and delivered panels to the active construction area. This operator, at times assisted by a laborer, also laid out the required panel types behind the wall face and at their approximate installation location. A second operator and two laborers worked with a hydraulic excavator to lift and set each panel in the design location on the wall. The installation was followed by two laborers who set wedges and braces to achieve the desired batter. The batter was typically very small (3–5 mm).

The reinforcing strip crew consisted of four to six laborers, an operator, and a foreman. The operator used a forklift fitted with a wide flange beam to transport the reinforcing strips. To prevent damage, the reinforcing strips were carried on the web of the wide flange beam. Laborers would then lift each strip off the beam and individually set them in the approximate installation location. Two laborers would next install the splice plates and tighten the bolts. The reinforcing strip manufacturer adopted lengths of up to 13.4 m (44 ft) thereby eliminating about 30,000 splices. The maximum reinforcing strip length was determined by galvanizing and shipping requirements.

The backfill crew consisted of three or four operators using bulldozers, a grader, and a Caterpillar model CS-563D vibratory roller to spread and compact the fill. The smooth 10,875-kg (24-kip) drum roller had a 1.55 m (61 in.) diameter, 2.13 m (84 in.) in width, and supplied static and dynamic compaction forces of 26.4 (148) and 127.5 kg/cm (714 lb/in.). A separate crew member directed the dump trucks to optimize backfill locations, avoid installed and exposed reinforcing strips, and help check grade.

Wall Performance

The west MSE wall was monitored at 10 stations along the 436 m (1,430 ft) length. The following observations are for the wall cross section located at Station 180+00, near the center of the wall. The performance observed at this location was relatively consistent with that at secondary instrumented sections located approximately 91.4-m (300-ft) north and south of Station 180+00. These secondary sections were at locations where the wall transitions to three tiers and were observed using optical survey and inclinometer arrays.

Vertical Displacements

The results of the wall face DMP and sondex settlement monitoring at the primary instrumented section are shown in Figs. 5 and 6. The elevations of the DMPs and sondex rings are shown in Fig. 2. The baseline survey of the Tier 1 DMPs was completed 2 days before the end of Tier 1 construction, and therefore the settlement data from these surveys are incomplete. However, the baseline surveys for instrumented panels erected in subsequent tiers were usually done within 10 days of the start of erection in each tier. The baseline readings of the sondex rings in the native foundation and subgrade improvement zones were made before the start of wall construction. Subsequent readings by the instrumentation contractor began at the start of Tier 3 construction; hence, the records of vertical displacements are incomplete.

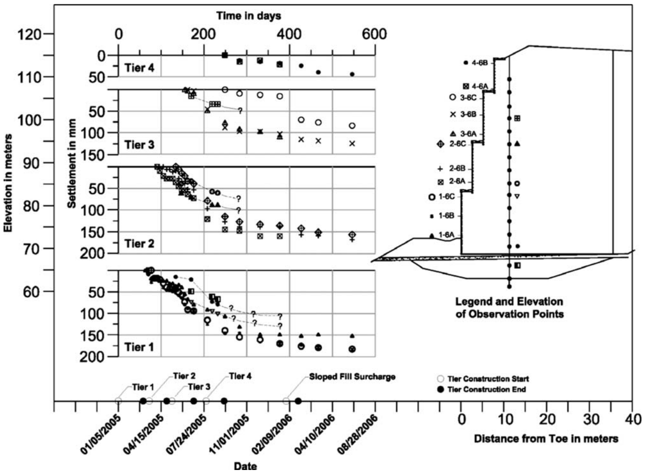

Fig. 5. Settlement time histories of the wall face, reinforced fill, and subgrade

Settlement Time History of the Wall Face

In general, construction of each tier resulted in approximately 50 mm of immediate settlement at the wall face of each underlying tier. In other words, the placement of Tiers 2, 3, and 4 resulted in approximately 150 mm (6 in.) in settlement at the top of Tier 1 (Fig. 5). The overall construction-related vertical strain between the top of the wall in Tier 4 and the top of the wall in Tier 1 is approximately 0.48%. Following completion of Tier 4, no additional fill was placed for 160 days. Over this time period settlement, as measured at individual DMPs located on the wall face, ranged from 12 to 43 mm (from 0.5 to 1.7 in.), with a trend of increasing settlement with depth below the top of the wall. The average strain for each tier over this time period is roughly 0.1%, estimated from measurements at the top and bottom DMP for each tier. It is noted here that outward lateral movement of the wall face, described below, over this time period likely contributed to the observed settlement.

Fill placement resumed on day 406. The placement of a 2H:1V surcharge above Tier 4 resulted in additional wall face settlement

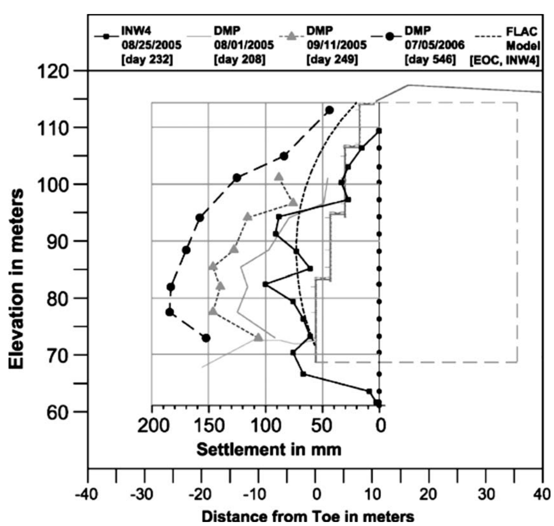

Fig. 6. Observed vertical displacement of the wall face within the reinforced soil and within the subgrade with FLAC model comparison

of 3–55 mm (0.1–2.2 in.) at the DMP locations. Final postconstruction settlement of the wall face, observed on day 546 (126 days following surcharge placement), ranged from 3 to 20 mm (from 0.1 to 0.8 in.). During the interval following the surcharge placement and the last settlement observation on day 546, the postconstruction strain averaged 0.05% within each tier. At the time of the last settlement observation, the mean vertical postconstruction strain rate within the reinforced fill had slowed to approximately 16 mm/year (0.6 in./year) and was continuing to slow. The settlement data corresponding to the lowest DMP at Tier 1 suggest that the densely compacted subgrade improvement zone and glacially overridden foundation soils did not creep.

Settlement Time History of the Subgrade and Reinforced Soil Mass

Settlement time histories below and within the reinforced soil mass are provided in Fig. 5 as measured at the inclinometer and sondex installation INW4. Unfortunately, no observations were made during construction of the first two tiers, limiting discussion of initial settlement behavior. Note that the last observation within the fill corresponds to day 232 when the fill was at approximately elevation 110 m (42 m or 138 ft tall). The settlement within the glacially overridden foundations soils, as indicated by the second sondex ring, was negligible, with observed data fluctuating within the error of the sondex sensor. For the subgrade improvement zone, little additional settlement accumulated with the placement of the two tiers following the completion of Tier 2. At day 232, during Tier 4 construction, the total amount of settlement within the subgrade improvement zone was 67 mm (2.6 in.). Although the manufacturer of the sondex probe suggests that the repeatability of the sondex measurements is typically ± 4 mm (0.15 in.), the comparison of the initial settlement within the subgrade improvement zone to that of the sondex rings suggests that the error may be larger. It is estimated that the final settlement within the subgrade improvement zone at day 546 was less than 125 mm (5 in.) or approximately 0.3% of the overall wall height by considering the increase in settlement observed at the bottom face of Tier 1 between days 232 and 546.

For clarity, only a portion of the sondex ring settlement time histories corresponding to the reinforced soils at INW4 are plotted in Fig. 5. These settlement time histories are applicable up to day 232 and therefore do not reflect the total settlements that occurred within the MSE wall fill. At day 232, settlement within the reinforced fill ranged from 10 to 100 mm (from 0.4 to 4 in.) or roughly 0.2% of the overall wall height.

Comparison of Settlement Profiles in Elevation

The settlements at the wall face and within the reinforced soil mass in elevation are shown in Fig. 6. The last sondex observation corresponds to day 232; the DMP settlement profiles, corresponding to days 208 and 249, are provided to bracket the sondex profile. The sondex profile indicates that the settlements at the top of each tier exceeded that observed at the bottom of the corresponding tier by approximately 25 mm (1 in.) for Tiers 1 and 2. Similarly, the settlements at the top of Tiers 1 and 2 are significantly larger than at the bottom of the next highest tier. The end-of-construction FLAC model prediction at the location of INW4 and final observed wall face settlement are also shown in Fig. 6. The observed settlements at day 232 or approximately 160 days prior to the placement of the sloped-fill surcharge generally follow the profile of the predicted settlements. However, it is expected that the settlements at INW4, had they been observed

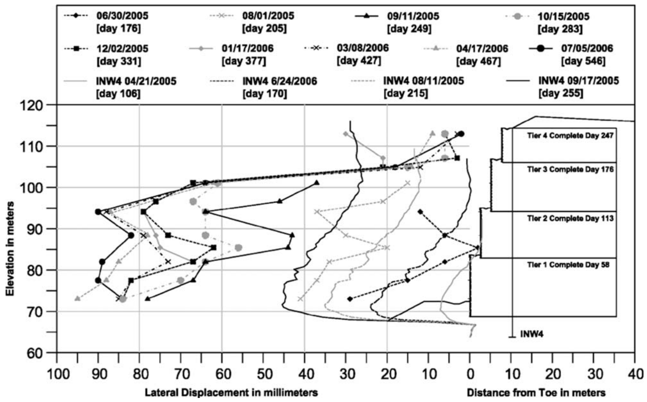

Fig. 7. Lateral displacement of wall face within the reinforced soil mass and within the subgrade

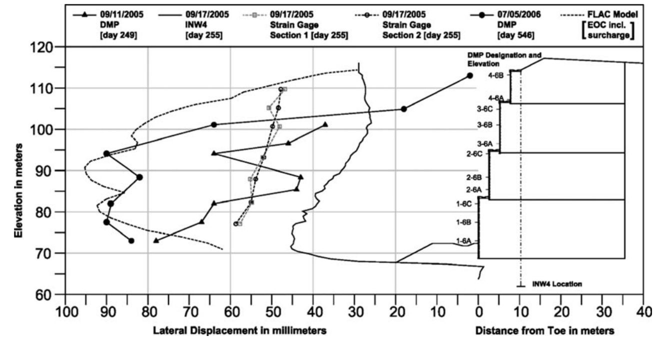

Fig. 8. Comparison of lateral displacement and integrated strain gauge observations prior to the placement of the sloped-fill surcharge and at end of construction with FLAC model comparison

following the placement of the remaining 4 m of wall and the sloped surcharge, would have exceeded that predicted end-of-construction FLAC model.

The profile of settlement at the wall face bracketing day 232 indicates that the wall face settled more than the reinforced fill behind. However, the profile of settlement at the wall face does not exhibit geometry-specific concentrations of settlement. It is noted that local rotations of the concrete facing panels may produce error within the optical survey of the wall face. The settlement profiles exhibit a roughly parabolic shape, in agreement with the observed performance of thick granular fills [e.g., Wilson (1973) and Charles (2008)].

Differential Settlement

The vertical displacements at the MSE wall face are greater than the settlements observed within the reinforced fill, with some potential and additional difference attributable to the delay in baseline survey of the DMPs. Near the end of wall construction (and prior to sloped surcharge placement), the settlement at the base of Tier 1 was approximately 35 mm (1.4 in.) greater than within the reinforced fill. Based on the settlement performance of Tier 1 due to placement of Tier 2, it is estimated that no more than 50 mm (2 in.) of settlement occurred at the wall face of Tier 1 due to construction of Tier 1. Therefore, a *maximum* of approximately 85 mm (3.4 in.) of differential settlement from the face of the MSE wall to the location of the inclinometer casing (approximately 11 m or 36 ft away) *may* have occurred by the end of wall construction.

The inherent structural flexibility of the MSE wall system is demonstrated by the *estimated maximum* angular distortion of approximately 1/125. In terms of settlement, the most critical wall performance factor was anticipated to be the differential settlement along the face of the wall. Remarkably, observations at the nine secondary instrumented sections indicate a maximum differential settlement of only 12 mm over 76.2 m or an angular distortion of less than 1/6,000. The west MSE wall has performed excellently in this regard.

Lateral Displacements

Lateral Displacements within the Reinforced Soil Mass

Lateral displacements within the reinforced soil mass were observed at inclinometer installations such as INW4, 2.44 m (8 ft) from the face of Tier 4 (Fig. 7). The INW4 profile of displacement, shown on Fig. 7, indicates an outward lateral soil movement of the lower portions of the reinforced fill and an apparent rotation of the higher portions of the wall (the upper part of Tier 3 and Tier 4) during construction of Tier 4. At the end of Tier 2 construction, the maximum lateral movement within the reinforced fill was approximately 8 mm (0.3 in.). Following Tier 2 construction, the maximum lateral movement at the inclinometer location increased at a rate of about 2.4 mm/m of fill (0.03 in./ft) to a maximum lateral displacement of 45 mm (1.8 in.) at the end of Tier 4 construction (September 2005). The maximum lateral wall displacement occurred just above the toe of the wall, with a roughly linear decrease of lateral displacement with increasing height to about the middle of Tier 3 after which the trend in lateral displacement reverses. The lateral displacement at this inflection point is approximately 26 mm (1 in.); lateral displacements increase with elevation to a maximum of approximately 30 mm (1.2 in.) at the top of the wall. The maximum lateral displacement observed within the reinforced soil mass, 45 mm, is approximately one-tenth and one-eighth of a percent of the wall height and base width, respectively, and was not considered excessive.

Lateral Displacements of the Wall Face

Lateral displacements of the wall face are also shown on Fig. 7 for time periods corresponding to the end of Tier 3 construction (day 176, June 2005), the start of Tier 4 (day 205, August 2005), the end of Tier 4 construction (day 249, September 2005), and for several intervals up to approximately 10 months after the end of wall construction (day 546, July 2006). Wall face surveys prior to the end of Tier 3 construction did not indicate significant face displacements. However, at the end of the Tier 3 construction (day 176), surveys of the wall face exhibited a profile of outward movement with the greatest displacement of approximately 30 mm (1.2 in.) near the base of the wall. The displacement profile indicates an irregular pattern of wall face displacement, possibly accentuated by the inherent flexibility of the wall facing panels. The wall face displacement continued to exhibit an irregular profile with the addition of Tier 4, the sloped-fill surcharge, and with creep through the last wall face survey (day 546). The final lateral displacement profile shows approximately 90 mm (3.5 in.) of displacement in Tiers 1 and 2, decreasing to about 20 mm (0.8 in.) at the top of Tier 3 with little observed movement at the top of Tier 4. Note that differential settlement between the wall face and points behind the wall face, as well as the sloped-fill surcharge, may have influenced the profile of lateral displacement.

Fig. 8 shows a comparison of the lateral displacements corresponding to the end of Tier 4 construction for the wall face survey, the inclinometer survey, and the integration of strain within the reinforcing strips. It also shows the end-of-construction displacement for wall face survey and those predicted by the FLAC model. The lateral movement within the reinforced soil at the end of Tier 4 construction measured by the inclinometer is approximately 5–30 mm less than that observed via the wall face survey. The displacement profile estimated with the FLAC model at the end of construction (following placement of the sloped-fill surcharge) is in good agreement with the final equilibrated displacement profile from the wall survey. The maximum observed lateral wall displacement, at 90 mm, is approximately 0.2% of the reinforced wall height. This value is about 25% of that predicted by the empirically based procedure recommended in AASHTO (2002).

In addition to the wall face survey, the strains within the reinforcing strips were integrated and added to the component of lateral wall movement at the base of the reinforced fill zone, following the method outlined by Stuedlein et al. (2007), to produce an independent estimate of wall face displacement (Fig. 8). Lateral movement at the base of the reinforced zone for the north MSE wall, which was observed at three inclinometer installations, was found to be relatively uniform across the foundation/wall interface (Stuedlein et al. 2007). At the west MSE wall, lateral displacement at the foundation/wall interface was observed to be approximately 40 mm at the location of INW4; this value was added to the integration of strains within the reinforcing strips, allowing an independent estimate of wall face displacement to be obtained. The displacement profile thus estimated and plotted in Fig. 8 indicates a slightly decreasing trend in wall face displacement with increasing height of wall with little variation between strips at a given elevation. The displacement profile falls within the bounds of the wall face survey for the same period.

Comparison of Vertical and Lateral Displacement Profiles

Assuming that the reinforced soil mass maintains constant volume, it can be shown that the vertical displacement in the settlement trough at the top of the wall (assumed equal in width to that of the active zone) is greater than the corresponding lateral displacement at the wall face. Fig. 9 compares the vertical and lateral profiles of displacement in elevation for INW4 at day 232 and the wall face at days 249 and 546. It is observed that the vertical displacements are consistently greater than lateral displacements at a given time period. Neglecting the top of Tier 4, the mean ratio of vertical to lateral displacement for each profile falls within the narrow range of 2.25–2.35, with coefficient of variation in ratio of 30–45%. The ratios of displacements correspond to a very high strength friction material consistent with that specified and placed within the MSE walls.

Reinforcement Strain and Inferred Stress Distribution

The distribution of strains and estimated stresses within the reinforced soil mass is plotted in terms of percent of yield stress in Fig. 10 for both instrumented sections. The results from the end-of-construction FLAC model are provided for comparison. The strain distributions within the sections are comparable to one another and generally less than that predicted by the numerical model. The measured strain distributions exhibit multiple instances of local maxima and minima. Reinforcing strips in the upper three tiers show a marked decrease in strain at a distance of approximately 13–21 m (42.7–68.9 ft) behind the toe of the wall.

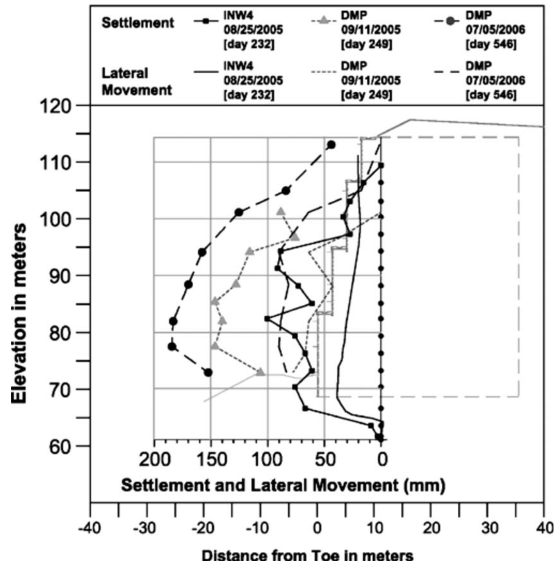

Fig. 9. Comparison of settlement and lateral movement at the wall face within the reinforced fill and within the subgrade prior to placement of the sloped-fill surcharge and at end of construction

Additional reductions in tensile strain are observed at distances ranging from 29 to 32 m (95.1 and 104.9 ft) behind the toe of the wall. Similar behavior was noted by Stuedlein et al. (2007), which was incorrectly attributed to potential initialization of shear localization thought to produce multiple surfaces of maximum shear strain within the fill potential differential settlement and the filling sequence for the north MSE wall.

Upon further study, the locations of local strain reductions were found to correspond with the locations of the reinforcing strip splices, provided in Table 2. The cross section of the splice plates, nuts, and bolt heads at the locations of the splices between

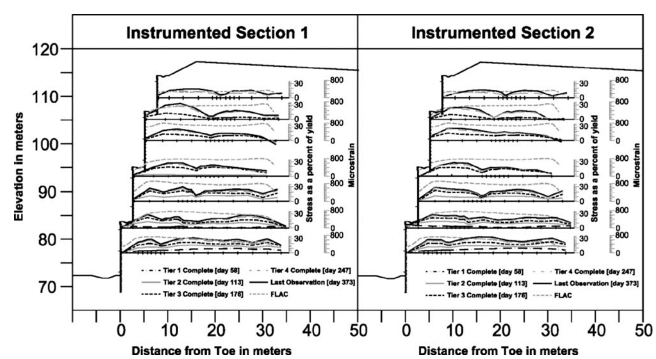

Fig. 10. Measured strain and estimated stress in reinforcement strips and FLAC model comparison; note that the surcharge fill was not completed until day 420

Table 2. Locations of Reinforcing Strip Splices

		Distance of splice behind toe of wall (m)	
Tier	Tier offset (m)	First splice	Second splice
1	0.00	13.41	26.82
2	2.44	15.85	29.26
3	4.88	18.29	31.70
4	7.32	20.73	34.14

individual lengths of reinforcing strip produces 1,910–2,130 mm^2 (3.0–3.3 $in.^2$) of bearing area. Lateral bearing is developed on the projected splice area similar to that developed on the transverse wires in welded bar mat reinforcements (Jewell 1980; Jewell et al. 1985; Palmeria and Milligan 1989). The field behavior of welded bar mats has been observed and documented by Anderson et al. (1987), Neely (1993), and others. The reduction in strain at the location of the splices reflects the fact that some load transfer occurs in lateral bearing rather than reinforcing strip-to-soil interface shear. The amount of tensile strain reduction is a function of confining stress and its role in controlling the amount and rate of dilation available for the clean granular backfill. Therefore, the reduction in reinforcing strip tensile strain, as a function of the depth from the top of the west MSE wall, increases to a maximum at a relatively shallow depth of approximately 9 m, subsequently decreasing with additional depth. Little strain reduction at the splice locations was observed along instrumented reinforcing strips in Tier 1.

Considering the peak strains closest to the wall face, the range in distance from the back of the wall to peak strain falls within 2.5–10.4 m (8.2–34.1 ft), with average and standard deviation of distance of 6 and 2.2 m (19.7 and 7.2 ft), respectively. With regard to the FLAC simulation, the reduction in strip thickness for metal loss allowance was incorporated in the model and may account for some of the difference between observed and predicted strains (i.e., overprediction of strains due to approximately 33% less steel in the FLAC model to account for the 100-year corrosion allowance). Other factors that may contribute to overprediction of reinforcement strain include potential three-dimensional effects, resulting in less reinforcement load demand, and/or the increased resistance to pullout of the strips due to the thickness of the splices; nonetheless, the reduced section area model likely provides the best explanation for overprediction of reinforcement strains by the FLAC simulation. Work is currently under way to present a more comprehensive evaluation of reinforcement strains, including a comparison of the maximum unit reinforcement load estimated from strain observations to the predictions resulting from the available design methods.

Summary and Conclusions

The west MSE wall for the third runway at STIA was constructed to avoid creek relocation and minimize wetland impacts. The design team selected steel strip reinforced earth technology based on past successful construction of tall MSE walls to limit the amount and extent of embankment fill. Good project team coordination, with oversight by a technical review board and other peer review, contributed to the successful completion of what is believed to be the tallest MSE wall in the western hemisphere. Geotechnical instrumentation, including wall surveys, inclinometer installations with sondex settlement rings, piezometers, and strain gages on reinforcing strips, provided the design and construction team with the information required to verify performance of the wall relative to design as construction progressed. The performance data of the west MSE wall provide insight into the behavior of very tall MSE walls and should provide useful reference data for future designers of MSE walls. The overall performance of the MSE wall as observed through the implemented geotechnical instrumentation is excellent.

Acknowledgments

The writers wish to thank the Port of Seattle, particularly the lead geotechnical constructor inspector, Dan Berta, and project manager, Scott Kyles, PE, for helping prepare critical information pertinent to the generation of this document. The writers acknowledge the significant contribution of HNTB, which provided project management and civil engineering for the MSE walls led by project manager Jim Thomson, PE. The writers thank the contractor's Instrumentation Engineer, P. Erik Mikkelsen, PE, and Instrumentation Specialist, Dave Yonemitsu, who recorded and provided the sondex settlement data. The writers also wish to express appreciation for design input from the Port's Technical Review Board which consisted of Peter Douglass, PE; Professor James Mitchell, PE; Professor Ed Idriss, PE; and Dr. Barry Christopher, PE. The writers extend gratitude to Dr. Stan Boyle, PE, Tony Allen, PE, and Professor Bob Holtz, PE, for discussions, comments, and suggestions.

References

AASHTO. (1996). *Standard specifications for highway bridges*, 16th Ed., American Association of State Highway and Transportation Officials, Washington, D.C., with interims.

AASHTO. (2002). *Standard specifications for highway bridges*, 17th Ed., American Association of State Highway and Transportation Officials, Washington, D.C., with interims.

Anderson, L. R., Sharp, K. D., and Harding, O. T. (1987). "Performance of a 50-foot high welded wire wall." *Proc., Soil Improvement—A Ten Year Update*, J. P. Welsh, ed., ASCE, New York, 280–308.

Bray, J. D., Augello, A. J., Leonards, G. A., Repetto, P. C., and Byrne, R. J. (1995). "Seismic stability procedures for solid waste landfills." *J. Geotech. Geoenviron. Eng.*, 121(2), 139–151.

Charles, J. A. (2008). "The engineering behaviour of fill materials: The use, misuse, and disuse of case histories." *Geotechnique*, 58(7), 541–570.

Chen, S. B., and Bailey, M. J. (2004). "Lessons learned from a stone column test program in glacial deposits." *GeoSupport 2004: Drilled shafts, micropiling, deep mixing, remedial methods, and specialty foundation systems*, J. P. Turner and P. W. Mayne, eds., ASCE, Reston, Va., 508–519.

Elias, V., Christopher, B. R., and Berg, R. R. (2001). "Mechanically stabilized earth walls and reinforced soil slopes—Design and construction guidelines." *FHWA-NHI-00-043*, Federal Highway Administration, Washington, D.C.

Fast LaGrangian Analysis of Continua (FLAC), version 4.0. (2000). Itasca Consulting Group, Inc., Minneapolis, Minn.

Galster, R. W., and LaPrade, W. T. (1991). "Geology of Seattle, Washington, United States of America." *Bull. Int. Assoc. Eng. Geol.*, XXVIII(3), 235–302.

Hudson, M., Idriss, I. M., and Baikae, M. (1994). *Quad4M user manual*, National Science Foundation, Washington, D.C.

Idriss, I. M., Lysmer, J., Hwang, R., and Seed, H. B. (1973). "Quad-4: A computer program for evaluating the seismic response of soil structures by variable damping finite element procedures." *Rep. No. EERC 73-16*, Univ. of California, Berkeley, Calif.

Jewell, R. A. (1980). "Some effects of reinforcement on soils." Ph.D. thesis, Univ. of Cambridge.

Jewell, R. A., Milligan, G. W. E., Sarsby, R. W., and Dubois, D. (1985). "Interaction between soil and geogrids." *Polymer grid reinforcement*, Thomas Telford, London, 18–30.

Leshchinsky, D., and Han, J. (2004). "Geosynthetic reinforced multitiered walls." *J. Geotech. Geoenviron. Eng.*, 130(12), 1225–1235.

Lindquist, D. D. (2008). "Seismic modeling of a 135-foot-tall MSE wall." *Soil dynamics IV*, ASCE, Reston, Va.

Makdisi, F. I., and Seed, H. B. (1978). "Simplified procedure for estimating dam and embankment earthquake-induced deformations." *J. Geotech. Geoenviron. Eng.*, 104(GT7), 849–867.

Morgenstern, N. R., and Price, V. E. (1965). "The analysis of the stability of general slip surfaces," *Geotechnique*, 15(1), 79–93.

Neely, W. J. (1993). "Field performance of a retained earth wall." *Renforcement des sols: Experimentations en vraie grandeur des annees 80*, Paris (in French), 171–200.

Negussey, D., and Stuedlein, A. W. (2003). "Geofoam fill performance monitoring." *Utah Dept. of Transportation, Rep. No. UT-03.17*, Salt Lake City, Utah, 45.

Newmark, N. M. (1965). "Effects of earthquakes on dams and embankments." *Geotechnique*, 15(2), 139–160.

Palmeria, E. M., and Milligan, G. W. E. (1989). "Scale and other factors affecting the results of pull-out tests of grids buried in sand." *Geotechnique*, 39(3), 511–524.

Peck, R. B. (1969). "Advantages and limitations of the observational method in applied soil mechanics." *Geotechnique*, 19(2), 171–187.

Proshake user manual. (2000). EduPro Civil Systems, Bellevue, Wash.

Sankey, J. E., Bailey, M. J., and Chen, B. S. (2007). "SeaTac third runway: Design and performance of MSE tall wall." *Proc. New Horizons in Earth Reinforcement*, J. Otani, Y. Miyata, and T. Mukunoki, eds., Taylor and Francis, London, 151–156.

Sankey, J. E., and Soliman, A. (2004). "Tall wall mechanically stabilized earth applications." *Geo-Trans 2004: Geotechnical engineering for transportation projects*, M. K. Yegian and E. Kavazanjian, eds., ASCE, Reston, Va., 2149–2158.

Seed, H. B., and Martin, G. R. (1966). "The seismic coefficient in earth dam design." *J. Soil Mech. and Found. Div.*, 92(SM6), 105–134.

Spencer, E. (1967). "A method of analysis of embankments assuming parallel interslice forces," *Geotechnique*, 17(1), 11–26.

Stuedlein, A. W., Mikkelsen, P. E., and Bailey, M. J. (2007). "Instrumentation and performance of the north safety area MSE wall, Sea-Tac International Airport." *Field measurements and geomechanics, GSP No. 175*, ASCE, Reston, Va.

Stuedlein, A. W., Negussey, D., and Mathioudakis, M. (2004). "A case history of the use of geofoam for bridge approach fills." *Proc., 5th Int. Conf. on Case Histories in Geotechnical Engineering*, S. Prakash, ed., Univ. of Missouri, 10.

User's guide, slope/W for stability analysis, version 4. (1998). Geo Slope International Ltd., Calgary, Alta.

Wilson, S. D. (1973). "Deformation of earth and rockfill dams." *Casagrande volume: Embankment dam engineering*, R. C. Hirschfeld and S. J. Poulos, eds., Wiley, New York, 365–417.